IOPscience iopscience.iop.org

Home Search Collections Journals About Contact us My IOPscience

Structure and dynamics of concentrated aqueous solutions of aluminium chloride, beryllium chloride and aluminium bromide: Raman, inelastic neutron scattering and x-ray diffraction results

This article has been downloaded from IOPscience. Please scroll down to see the full text article.

2004 J. Phys.: Condens. Matter 16 6343

(http://iopscience.iop.org/0953-8984/16/36/002)

View the table of contents for this issue, or go to the journal homepage for more

Download details:
IP Address: 129.252.86.83
The article was downloaded on 27/05/2010 at 17:24

Please note that terms and conditions apply.

J. Phys.: Condens. Matter **22** (2010) 149801 (1pp) doi:10.1088/0953-8984/22/14/149801

Corrigendum

Structure and dynamics of concentrated aqueous solutions of aluminium chloride, beryllium chloride and aluminium bromide: Raman, inelastic neutron scattering and x-ray diffraction results
A M Gaspar, M Alves Marques, M I Cabaço, M I de Barros Marques, A I Kolesnikov, J Tomkinson and J-C Li 2004 *J. Phys.: Condens. Matter* **16** 6343–6364

Recently the following inaccuracies have been detected in the above article:

- On page 6349, the second line from the bottom $x_t^{H_2O}$ should read $\xi_t^{H_2O}$.
- In appendix A, line 4 u1 should read v_1.
- In table 4, the caption of the last column $\xi_t^{H_2O}/\xi_t^{D_2O}$ should read $\xi_t'^{H_2O}/\xi_t'^{D_2O}$.
- In table 4, under 'Degenerate vibrations' the entries in the eighth column should be transposed with those in the ninth column. Hence, the value 431.5 in the eighth column should read 324.0 and the value 324.0 in the nineth column should read 431.5. Similarly, 474.5 in the eighth column should read 325.6 and 325.6 in the nineth column should read 474.5.

The authors regret any inconvenience these inaccuracies might have caused.

 © 2010 IOP Publishing Ltd Printed in the UK & the USA

INSTITUTE OF PHYSICS PUBLISHING JOURNAL OF PHYSICS: CONDENSED MATTER

J. Phys.: Condens. Matter **16** (2004) 6343–6364 PII: S0953-8984(04)81476-0

Structure and dynamics of concentrated aqueous solutions of aluminium chloride, beryllium chloride and aluminium bromide: Raman, inelastic neutron scattering and x-ray diffraction results

A M Gaspar[1,2], M Alves Marques[1,2], M I Cabaço[1,2], M I de Barros Marques[1,2], A I Kolesnikov[3], J Tomkinson[4] and J-C Li[5]

[1] Centro de Física Atómica, Avenida Professor Gama Pinto 2, 1649-003 Lisboa, Portugal
[2] Departamento de Física do Instituto Superior Técnico, Avenida Rovisco Pais, 1049-001 Lisboa, Portugal
[3] Intense Pulsed Neutron Source, Argonne National Laboratory, Argonne, IL 60439, USA
[4] CCLRC, The Rutherford Appleton Laboratory, Chilton OX11 0QX, UK
[5] Department of Physics, UMIST, PO Box 88, Manchester, M60 1QD, UK

E-mail: agaspar@cii.fc.ul.pt

Received 1 June 2004
Published 27 August 2004
Online at stacks.iop.org/JPhysCM/16/6343
doi:10.1088/0953-8984/16/36/002

Abstract

Structural and dynamical investigations on concentrated aqueous solutions of aluminium chloride and bromide in liquid and glassy states have been performed by means of Raman and inelastic neutron scattering spectroscopy and by x-ray diffraction. Inelastic neutron scattering results for solutions of beryllium chloride in a glassy state are compared with the results for the aluminium cation solutions. Isotopic changes on going from H_2O to D_2O of the Raman spectra assigned to vibrations of water molecules in the cation hydration shells are discussed. Inelastic neutron scattering data complement and corroborate the Raman spectral study. Further structural information is obtained from x-ray diffraction experiments, and its interpretation is supported by calculations based on ad hoc molecular models. The existence of a *liquid-type quasi-close packing* is suggested for concentrated aqueous solutions of aluminium halides, in agreement with previous studies.

1. Introduction

The structure and dynamics of liquid water and aqueous solutions are of interest both for fundamental research and for many technological applications, which require a deep insight into these properties. So this knowledge is of particular relevance in biology and environmental

 © 2004 IOP Publishing Ltd Printed in the UK

sciences. In this contribution we stress a plausible connection between the possibility of the existence of positional correlations between hydrated ions, induced by mutual electrostatic interactions, and their ability to coordinate a large number of water molecules. The persistence of the hydration shells had already been detected by Raman spectroscopy experiments with different aqueous solutions containing the same ions. These studies can lead to relevant information on the behaviour of the water molecule in condensed states of matter. The small, highly charged aluminium and beryllium cations appear to be good choices for illustrating the importance of electrostatic interactions.

Raman experiments on concentrated aqueous solutions of aluminium and beryllium halides have previously been reported by some of the authors of this paper [1–3] and reviewed [4]. These previous studies [1–4] suggested the existence of local hydration structures around the cations in the liquid state at room temperature. Inelastic neutron scattering experiments, described in the second section, show similar local structures in the corresponding glassy solutions at low temperature. At low temperature, quasi-elastic neutron scattering effects due to diffusion processes are reduced, allowing more detailed analysis of the weak activity in the low frequency region. Moreover, vibrational modes inactive in Raman spectroscopy are active in inelastic neutron scattering, permitting a more detailed interpretation of the vibrational spectra of these local structures. This complementary information suggested to the authors that the interpretation of the Raman spectra ought to be re-examined. The existence of positional correlations between these local hydration shells is discussed in the last section, on the basis of the results from x-ray diffraction studies on concentrated aqueous solutions of aluminium halides. The structures observed in the liquid state at room temperature appear to be very similar to those seen in the glassy state. In this state the previously reported [5] existence of positional correlations between aluminium hydrates was carefully analysed. The hypothesis of any significant coupling between vibrational modes of neighbouring hydrates was rejected since the mean distance between close cations is two or three times greater than the mutual distances between coordinated water molecules inside the hydrate.

Briefly, Raman spectroscopy can detect the presence of the highly polarizable electron clouds of the oxygen atoms or ions, neutron scattering studies demonstrate the relevance of the hydrogen atoms when, in experiments, the hydrogen–deuterium contrast is appropriate for obtaining conclusions, and x-ray diffraction is used here to identify cation and anion positions by comparing the patterns for two solutions where chloride and bromide anions occupy similar positions.

2. Experimental details

The aqueous solutions were prepared by weight, dissolving commercially available salts in bidistilled water or in deuterium oxide. Hydrated aluminium and beryllium nitrates, anhydrous aluminium and beryllium chloride and deuterium oxide were obtained from Merck–Schuchardt ($D_2O > 99.75\%$), while anhydrous aluminium bromide was obtained from Aldrich. The compositions of the aqueous solutions investigated, which were monitored via chemical analysis, are presented together with the corresponding densities in table 1.

The aqueous solutions for Raman spectroscopy were filtered through nitrocellulose membranes prepared in our laboratory, to reduce the background in the spectra due to impurities of the solution. The presence of HDO or ordinary water in the deuterium oxide solutions was monitored via the intensity of the Raman spectra in the region of the corresponding intramolecular Raman bands. For the inelastic neutron scattering experiments the aqueous solutions in deuterium oxide were prepared and kept under argon until the experiment was performed to avoid any contamination with hydrogen. Vitrification of a sample solution was

Table 1. The composition, density and molar concentration of the aqueous aluminium and beryllium halide solutions investigated. n is the number of water molecules per cation.

Salt	n	$d_{20\,^\circ C}$ (g cm^{-3})	m (mol dm^3)
$AlCl_3$	$16.4H_2O$	1.329	3.09
	$18H_2O$	1.309	2.86
	$24H_2O$	1.240	2.19
	$30H_2O$	1.191	1.77
	$18D_2O$	1.394	2.82
$AlBr_3$	$18.0H_2O$	1.586	2.67
	$24H_2O$	1.456	2.08
	$30H_2O$	1.377	1.71
	$18D_2O$	1.701	2.71
$Al(NO_3)_3$	$18.4H_2O$	1.387	2.55
$BeCl_2$	$6H_2O$	1.344	7.15
	$12H_2O$	1.198	4.05
	$12D_2O$	1.290	4.03
$Be(NO_3)_2$	$11.4H_2O$	1.317	3.90

achieved by immersing the filled sample container in liquid nitrogen; the cool down time was about 2 min.

Raman spectra were obtained with a Renishaw 1000 spectrometer using the 514.5 nm line of an Ar^+ laser and the backscattered light was detected by a CCD system. The overall spectral resolution was $\sim$3 cm^{-1}. Aqueous solutions were contained in 10 mm internal diameter borosilicate glass cylindrical cells with 2 mm thick flat windows. The cooling system involved a continuous liquid nitrogen flow cryostat, allowing minimal temperatures of $\sim$77 K. The vacuum tail had 1 mm thick, fused quartz windows. Spectra of the liquid samples were obtained at room temperature, while those of glassy samples were obtained at liquid nitrogen temperature.

Inelastic neutron scattering experiments were performed at the ISIS pulsed neutron source (Rutherford Appleton Laboratory, UK), using the TOSCA time-of-flight inverse-geometry spectrometer [6]. Spectra were obtained by counting neutrons, from a white pulse, and scattered by the sample with a given final energy ($\sim$4 meV) to detectors placed at a fixed scattering angle ($\sim$135°). These conditions imply different values of momentum transfer associated with different values of energy transfer, with Q^2 values increasing almost linearly from $\sim$12.5 Å^{-2} close to the elastic line to $\sim$120 Å^{-2} for 200 meV energy transfer. The samples were placed in aluminium planar cells with 0.5 mm thick walls, protected against chemical attack from aqueous solutions by nickel and gold coating. The sample thickness was set to 0.3 mm for solutions in ordinary water or to 3 mm for solutions in deuterium oxide. The cooling system was a closed-cycle He refrigerator. All the spectra of the glassy state were obtained at $T < 25$ K. Data processing included corrections for the energy distribution of the incoming neutron flux as well as conversion of the spectra for representation as functions of energy transfer, and was done using standard programs available at ISIS.

X-ray diffraction experiments were performed at the European Synchrotron Radiation Facility (ESRF, Grenoble) on the high energy beamline ID15b. Monochromatic synchrotron radiation of high energy (88.54 keV, 0.140 Å) was used. Samples were studied by means of transmission in 2 mm layers contained in plane parallel cells between Kapton windows (25 μm). A closed-cycle He refrigerator was used to obtain the x-ray diffraction pattern of

a glassy sample, allowing sample temperatures between 11 and 300 K. The vacuum chamber had Mylar windows (100 μm) for the incident and scattered x-rays.

The detection system was a MAR online image plate scanner (2300 × 2300 pixels, pixel size 0.15 mm). The one-dimensional diffraction patterns were obtained by integration of the diffraction rings of the 2D patterns. To gather information over the Q region of interest the x-ray diffraction patterns were acquired at two different distances from the sample to the detector: 320 and 960 mm. A tube filled with helium was used to significantly reduce the contribution from air scattering to the measurements at the longest path between the sample and the detector.

Corrections were made for the empty container, air (and helium) scattering contributions, absorption and geometry. For all the ions, the coherent scattering factors f_j were taken from x-ray tables [7] and corrected for anomalous scattering [8]. Incoherent scattered intensities corrected for the Breit–Dirac recoil factor were calculated from data from Palinkas *et al* [9] for the Cl^- and Al^{3+} ions and from Cromer *et al* [10] for the Br^- ion. For water molecules we used the coherent scattering factors and the incoherent scattered intensities from Hadju [11]. The corrected intensities were scaled to absolute units using the Krogh-Moe method [12]. Finbak's method, as reformulated by Warren [13], was applied to the experimental data and used to calculate the following total pair correlation function of the solution, $g(r)$:

$$g(r) = 1 + \frac{1}{2\pi^2 r \rho_e \sum_{uc} Z_j} \int_0^{Q_{max}} Q i'(Q) e^{-bQ^2} \sin Qr \, dQ \tag{1}$$

where ρ_e is the average electron density of the solution, Z_j are the atomic numbers and $i'(Q)$ is the reduced intensity defined as

$$i'(Q) = \frac{I_{eu}(Q) - \sum_{uc} f_j^2}{F^2(Q)} = \frac{i(Q)}{F^2(Q)} \tag{2}$$

where $F(Q) = \frac{\sum_{uc} f_j}{\sum_{uc} Z_j}$, $I_{eu}(Q)$ is the total intensity and $i(Q)$ is the so-called dependent intensity. The units of composition, uc, are always given with reference to the aluminium ion.

In the sharpening factor $F(Q)$, the sum extends over all three species in the solution (cation, anion and water molecules). Different values of Q_{max} were tested for both the Krogh-Moe method and the Fourier inversion. In the data analysis presented here we used Q values up to 18 Å^{-1}. For that value of Q_{max}, in the modification function e^{-bQ^2}, b was set equal to 0.006 Å^2. The cut-off produces spurious peaks and decreases the spatial resolution, but this is not relevant for distances greater than 1 Å. A final correction has been made reducing the spurious oscillations in the pair correlation function $g(r)$ at small distances (less than 1 Å). The so-called pair correlation function $g(r)$ was then back-transformed in order to obtain the corrected dependent intensity.

3. Results and discussion

3.1. Raman scattering investigations

The existence of a hydration structure around the aluminium cation independent of the anion has long [1–3] been suggested from results of Raman spectral studies on concentrated aqueous solutions of various salts. These spectra exhibit three bands in the low frequency region, which were initially attributed by Silveira *et al* [1, 2] to the Raman active vibrations of an octahedral hydration structure (figure 1).

Similar Raman investigations on concentrated aqueous solutions of beryllium salts suggested [2] the existence of a tetrahedral hydrate, in agreement with the results obtained by means of NMR [14]. Later NMR [15, 16] and x-ray diffraction [17] investigations

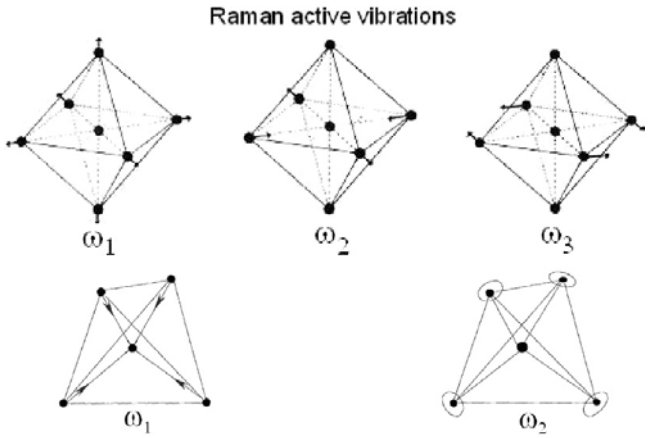

Figure 1. Raman active vibrations of octahedral and of tetrahedral aggregates.

permitted confirmation of a similar interpretation. The existence of six water molecules coordinated by the Al^{3+} cation in aqueous solutions was confirmed by the results of NMR [14–16, 18–20] and x-ray diffraction [21, 22] experiments and the stability of this species has been discussed [23–26]. More recently, aluminium hydrate has been the subject of other spectroscopy investigations [27–30]. In investigating different interactions between the aluminium cation and the water molecules belonging to its solvation shell, several *ab initio* calculations were implemented [31–40]; *ab initio* studies were performed also on the beryllium cation hydrate [31–33, 36, 41–45].

The cation with its hydration shell is considered here as a stable aggregate whose internal vibrations can be studied independently from the rest of the solution. This structure provides a satisfactory simulation for some results obtained by Raman spectroscopy. However, although interactions with water molecules of the second hydration shell cannot be strictly excluded, those with neighbouring hydrates seem less important for interpreting the profile of the Raman spectra. In this study we will not discuss the modification of the internal vibrations of the water molecule.

In the case of aluminium hydrates with six water molecules in an octahedral arrangement, only three vibrations of the internal modes are Raman active (figure 1)[6]. In the same figure, the two Raman active vibrations ω_1 and ω_2 of the T_d regular tetrahedral hydrate of the beryllium cation are shown.

The Raman spectra obtained for concentrated aqueous solutions of aluminium chloride and of aluminium bromide are compared in figure 2. The Raman spectrum obtained for a concentrated aqueous solution of beryllium chloride is given in figure 3. The Raman active bands are observed at the same frequencies, 524, 440 and 332 cm^{-1}, for the two solutions, in agreement with previous Raman studies [28], also shown in table 2. The small numerical differences are within experimental error. The frequencies of the Raman bands assigned to the vibrations ω_1 and ω_2 of the beryllium hydrate were 529 and 348 cm^{-1}. The frequency values of the Raman bands observed for concentrated aqueous solutions of aluminium nitrate in both the liquid and the glassy states (figure 4) are practically the same as those for the chloride and bromide (figure 2). The similarities in the spectra for the aluminium and beryllium hydrates as well as their nitrates in the liquid and glassy states (figures 4 and 5) suggest similar local environments. Similar behaviour has been found with concentrated aqueous solutions of indium and of lanthanum nitrate.

[6] The vibrational motions are referred to as ω_i, the corresponding Raman bands as ν_i and the frequency values as ξ_i.

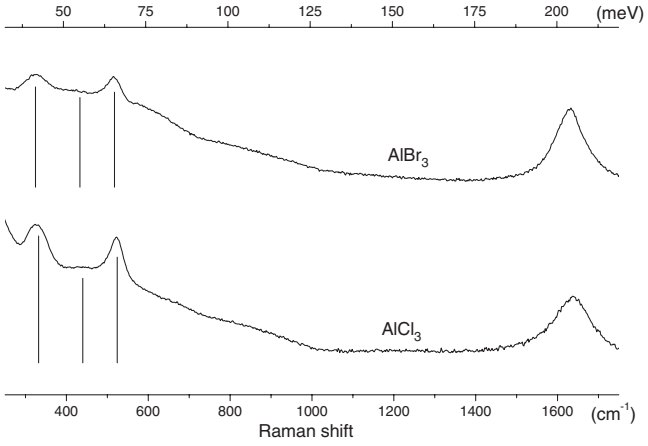

Figure 2. Raman spectra of concentrated aqueous solutions of aluminium chloride and bromide ($18H_2O/Al^{3+}$). The vertical lines indicate the frequency values 332, 440 and 524 cm^{-1}.

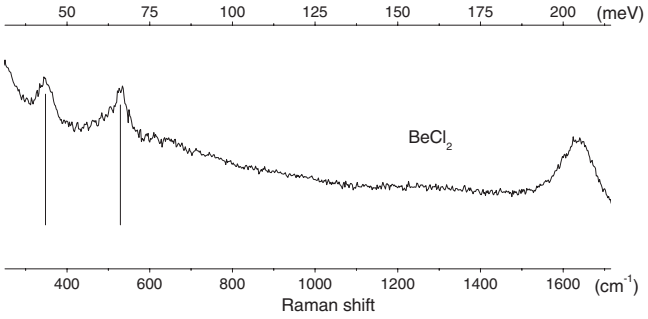

Figure 3. The Raman spectrum of a concentrated aqueous solution of beryllium chloride ($12H_2O/Be^{2+}$). The vertical lines indicate the frequency values 529 and 348 cm^{-1}.

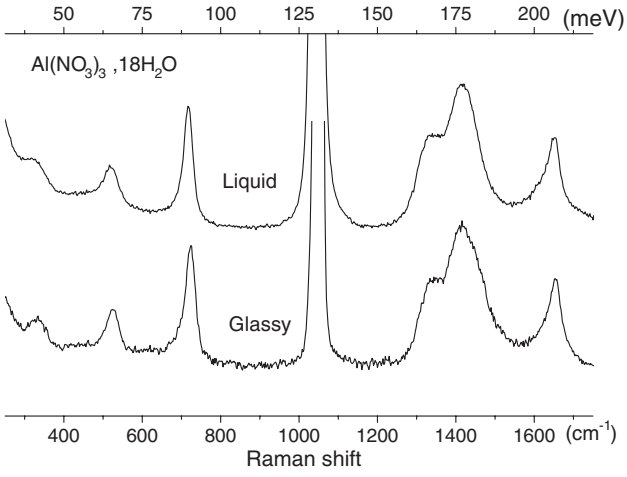

Figure 4. Raman spectra of concentrated aqueous solutions of aluminium nitrate ($18H_2O/Al^{3+}$) obtained at room temperature (liquid) and at 77 K (glassy). The spectra are similar.

In figure 6, the isotopic changes are shown for the spectra of aluminium chloride solutions on replacing H_2O with D_2O. The aluminium hydrate bands shift to 504, ∼420 and 312 cm^{-1}, while for beryllium hydrate shifts to 510 and ∼327 cm^{-1} were observed.

The isotopic shift $ish = \xi^{H_2O}/\xi^{D_2O} = 1.04$ obtained for the polarized band (corresponding to the vibration ω_1) is lower than expected from its original attribution to the totally symmetric vibration of the octahedral (or tetrahedral) hydrate. In this vibration only

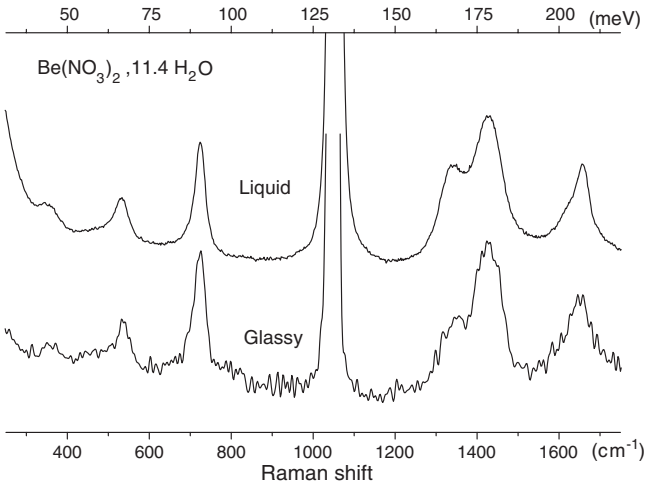

Figure 5. Raman spectra of concentrated aqueous solutions of beryllium nitrate ($11.4H_2O/Be^{2+}$) obtained at room temperature (liquid) and at 77 K (glassy). The spectra are similar.

Table 2. Comparison of the values of the frequencies of the bands observed in the inelastic neutron scattering spectra of concentrated aqueous solutions of aluminium and beryllium halides in the glassy state with the values of the bands observed in the Raman spectra of solutions of the same salts in the liquid state. n is the number of water molecules per cation, ish means isotopic shift. For the maxima of intensity observed in the spectra, that are assumed to correspond to the same vibrational modes, the values of the frequency that are obtained for the INS in the glassy state are not strictly coincident with the values measured in the Raman experiments with liquid solutions. This disagreement is probably related to the fact that each of these experimental scattering techniques probes different physical properties of the scatter samples, as we discuss at the end of the introduction.

INS glassy state			Raman liquid state (previous work [28])			
Salt	n	Freq. (cm^{-1})	Salt	n	Freq. (cm^{-1})	Freq. (cm^{-1})
$AlCl_3$	$16.4H_2O/Al^{3+}$	$\xi_3 \ldots 346$	$AlCl_3$	$16.4H_2O/Al^{3+}$	$\xi_1 \ldots 524$	$\xi_3 \ldots 329$
	$18H_2O/Al^{3+}$	353		$24H_2O/Al^{3+}$	524	336
	$24H_2O/Al^{3+}$	350		$40H_2O/Al^{3+}$	526	337
	$30H_2O/Al^{3+}$	363		$17.2D_2O/Al^{3+}$	503	310
	$18D_2O/Al^{3+}$	318			$ish(\nu_1) \sim 1.04$	$ish(\nu_3) \sim 1.06$
		$ish(\nu_3) \sim 1.10$		$22.0D_2O/Al^{3+}$	$\xi_1 \ldots 505$	$\xi_3 \ldots 317$
$AlBr_3$	$18H_2O/Al^{3+}$	$\xi_3 \ldots 352$			$ish(\nu_1) \sim 1.04$	$ish(\nu_3) \sim 1.06$
	$24H_2O/Al^{3+}$	346			$\xi_1 \ldots 507$	
	$30H_2O/Al^{3+}$	355			$ish(\nu_1) \sim 1.04$	
	$24D_2O/Al^{3+}$	317				
		$ish(\nu_3) \sim 1.20$				
$BeCl_2$	$6H_2O/Be^{2+}$	$\xi_2 \ldots 347$	$BeCl_2$	$<7H_2O/Be^{2+}$	$\xi_1 \ldots 527$	$\xi_2 \ldots 340$
	$12H_2O/Be^{2+}$	363		$27H_2O/Be^{2+}$	531	356
	$12D_2O/Be^{2+}$	340		$9.3D_2O/Be^{2+}$	508	320
		$ish(\nu_2) \sim 1.07$			$ish(\nu_1) \sim 1.04$	$ish(\nu_2) \sim 1.06$
				$27D_2O/Be^{2+}$	512	334
					$ish(\nu_1) \sim 1.04$	$ish(\nu_2) \sim 1.07$

a translational mode of the coordinated water molecule was assumed to be involved, so the ratio $x_t^{H_2O}/\xi_t^{D_2O}$ for the aluminium and beryllium hydrates should be given by the square root of the ratio of the isotope water molecules masses, 1.054 (see the inset of figure 6 and table 2).

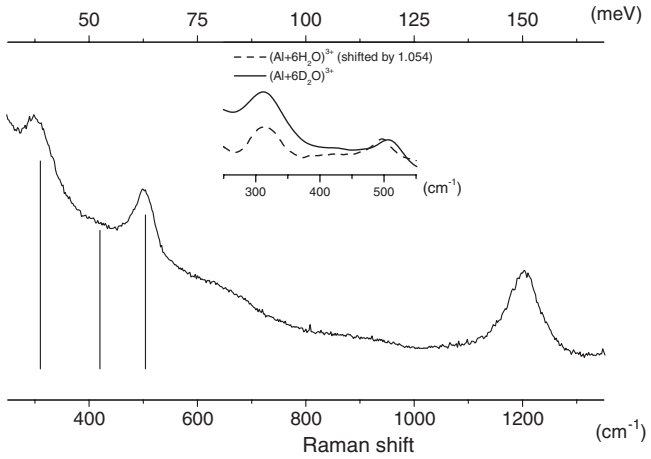

Figure 6. Raman spectra of aluminium chloride in deuterium oxide ($18D_2O/Al^{3+}$). The vertical lines indicate the frequency values 312, 420 and 504 cm^{-1}. The dashed curve in the inset was obtained by rescaling the spectrum of the aluminium chloride in ordinary water ($18H_2O/Al^{3+}$) by a factor of 1.054.

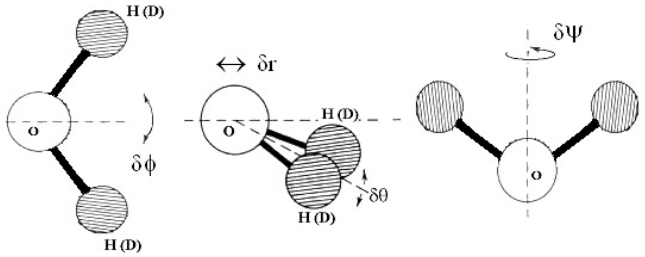

Figure 7. A schematic representation of the librational motions of the water molecules. $\delta\phi$ represents the rocking, $\delta\theta$ represents the wagging and $\delta\psi$ represents the *twisting* libration. δr represents the contraction–dilation of the cation–oxygen bond. As already mentioned, the cation is considered to be in the bisector plane of each coordinated water molecule with a non-zero value for the angle between the symmetry axis of the water molecule and the cation–oxygen bond.

This apparent discrepancy, revealed by the improved accuracy of the experimental observations, has already been noted [46] and is confirmed by these experiments. The hypothesis of pure translational vibrations must, therefore, be rejected. The isotopic shift 1.064, observed for the bands ν_2 (Be^{2+}) and ν_3 (Al^{3+}), when ordinary water is replaced by deuterium oxide has not yet been analysed. To interpret the experimental isotopic shift, we suggest that the vibration that leads to the band ν_1 in aluminium and beryllium solutions may be simulated, approximately, by coupling of a pure translational vibration with one of the hindered rotations [46, 47] of the coordinated water molecule (figure 7). This interpretation has previously been suggested [28] but is re-examined now using a coupling of the modes involving a configuration of the hydrate which is not the same as that used in the previous article.

The cation is considered to be in the bisector plane of each coordinated water molecule with a non-zero value for the angle between the symmetry axis of the water molecule and the cation–oxygen bond. As a consequence of this configuration, a preferential coupling of

the *wagging* libration with the pure translational vibration of the coordinated water molecules seems very plausible, although there may be a small coupling also with the other two librational modes.

Although in hydration structures of other cations, tilt angles have been suggested from experiment [48–54], this is not the case with either the aluminium or the beryllium cation, and for the aluminium cation the tilt angle is only suggested from calculations [34, 37, 39, 40].

In this analysis we consider as predominant the coupling of the totally symmetric translational vibration of the hydrate with one librational mode, the wagging. As a consequence of this coupling, which is assumed to be small, two vibrational modes are present: one predominantly translational, producing the polarized Raman band observed with both cation hydrates, and the other predominantly librational, which will be practically inactive in the Raman spectrum. The frequencies of both resultant modes are, obviously, not very different from those before coupling.

Although, as discussed above, the predominantly librational vibration resulting from this coupling is not detectable by Raman spectroscopy, it should be possible, in principle, to detect its activity by inelastic neutron scattering spectroscopy, since no selection rules exist. However, an unambiguous identification of that librational vibration is not possible. As a matter of fact, a Raman activity of other vibrations of water molecules and ions occurs in the range from $\sim$400 cm^{-1} up to $\sim$1000 cm^{-1}. This overlap is re-examined in the next section concerning inelastic neutron scattering.

The isotopic shift of the polarized Raman bands of the aluminium and beryllium hydrates is satisfactorily interpreted if the value of the wagging frequency is within the range $\sim$550 to $\sim$650 cm^{-1}. As a consequence of the above hypothesis of a preferential coupling with the wagging librations of the water molecules of the cation hydrates, we suggest that this vibration has a frequency somewhere in this interval. Slight couplings with other librational modes do not weaken this interpretation (see table 4, appendix A).

The existence of librational modes in the above range also allows an interpretation of the values of the isotopic shifts observed for the Raman bands attributed to the degenerate vibrations of the cation hydrates. Numerical examples with ad hoc values for the coupling parameters of the different librational modes are given in appendix A to illustrate this. At this stage of the knowledge of the structure of the water molecule, if bound in a hydration shell, accurate values cannot be given for these parameters.

3.2. Inelastic neutron scattering investigations

In inelastic neutron scattering spectra, the intensity associated with a given fundamental excitation (j) of the structure under investigation is proportional to

$$I_j \propto Q^2 x_j^2 \mathrm{e}^{-Q^2\langle x^2\rangle}\sigma \tag{3}$$

where x_j represents the amplitude of vibration of the atoms undergoing the j mode of vibration, σ is the neutron scattering cross section of the atoms involved in the mode, Q is the momentum transfer and the exponent is the Debye–Waller factor in which $\langle x^2\rangle$ represents the mean square displacement of the atoms in the scattering system. In figure 8(a), inelastic neutron scattering spectra of concentrated aluminium chloride aqueous solutions in liquid and glassy states are presented. The spectrum of the glassy sample is very similar to that of the liquid sample, which again suggests very similar structural arrangements of the atoms and molecules in the two states.

The room temperature data are less well defined on account of the large values of the mean square displacements of the ions and molecules (in the liquid state). In addition to this, a quasi-elastic component is observed in the low energy part of the spectrum due to the diffusion

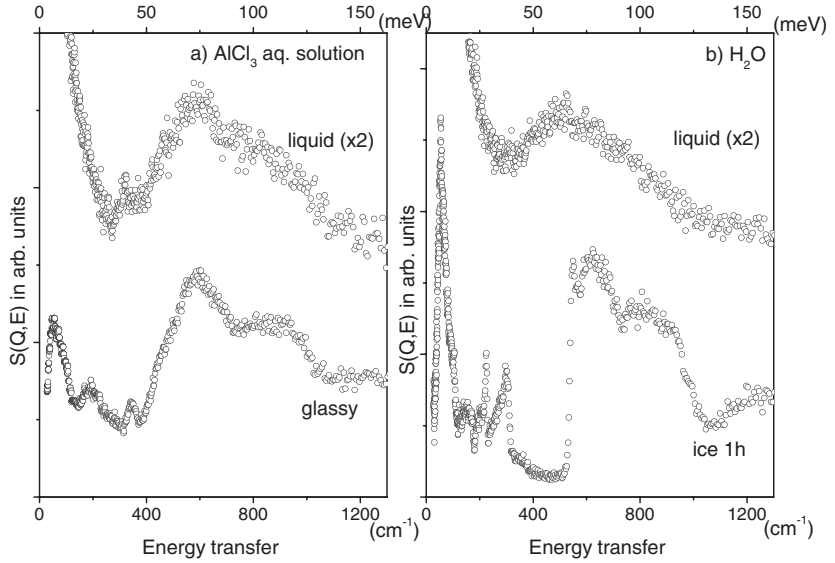

Figure 8. Inelastic neutron scattering spectra as measured on TOSCA at room temperature and at 20 K. (a) Concentrated aluminium chloride aqueous solution ($16.4H_2O/Al^{3+}$); (b) pure ordinary water (liquid and ice Ih).

processes occurring in the liquid sample and masking the fundamental inelastic component of the spectra. Consequently, a direct comparison between the spectra of concentrated aqueous solutions and that of pure liquid water is not easy, since very different diffusion values arise in the two systems [26, 55]. However, in the spectra obtained at about 20 K, diffusion effects are greatly reduced, leading to a much better defined profile, revealing the inelastic activity in the low frequency region. At high energy transfer, the suppression of the inelastic spectra is still observed and the reasonable 'multiphonon' contributions should also be considered.

In the case of pure water (figure 8(b)), the spectra of any ice phases [56] can be characterized by two distinct regions: one, below $\sim$300 cm^{-1}, related to the predominantly translational vibrations of the water molecules; and the other, starting at $\sim$400 cm^{-1} and extending up to $\sim$1000 cm^{-1}, related to the predominantly librational motions [47, 48]. This is suggested by the isotopic shift of these bands when deuterium oxide is used instead of ordinary water [56]. For ionic aqueous solutions the observed spectra must be regarded as the superposition of the vibrations of at least two kinds of water molecules: the water molecules belonging to the cation hydrate and the non-coordinated (*free*) water molecules. The water molecules of this second type, more numerous than those of the cation hydrates, will be responsible, certainly, for more than 50% of the intensity of the detected signal. The spectra of the different concentrated aqueous solutions are now compared among themselves and with those obtained in Raman experiments. The following comments are relevant:

(1) The inelastic neutron scattering profiles of solutions with a common cation are similar, in agreement with Raman data (figure 9). In the same figure the differences, relative to what is observed for pure water, of the profile of the scattering functions $S(Q, E)$ seem to be mainly determined by the cation. Some slight differences in the spectra of the aqueous solutions of aluminium bromide and aluminium chloride are visible below 700 cm^{-1} in the case of ordinary water solutions and below 500 cm^{-1} in the case of deuterium oxide solutions.

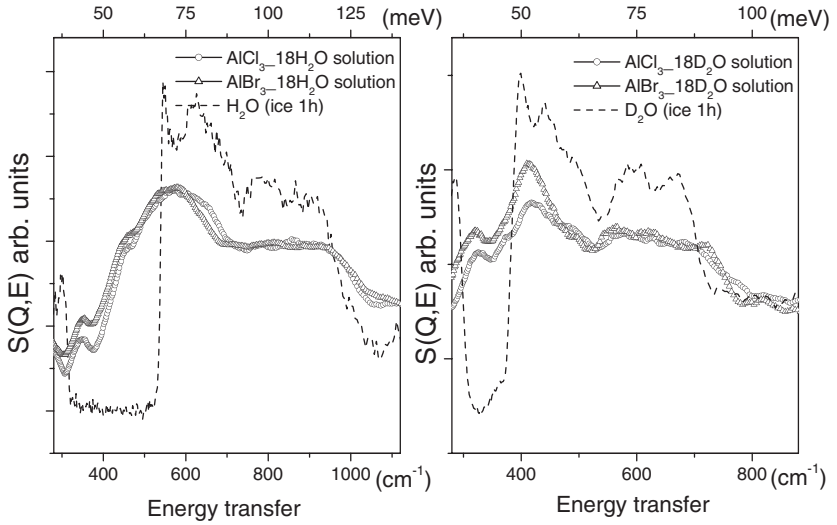

Figure 9. Inelastic neutron scattering spectra of concentrated aqueous solutions of aluminium chloride and aluminium bromide in ordinary water and in deuterium oxide ($18H_2O/D_2O$ per Al^{3+}) in the glassy state ($T < 25$ K). Dashed curves represent the ordinary pure water and deuterium oxide spectra (ice Ih).

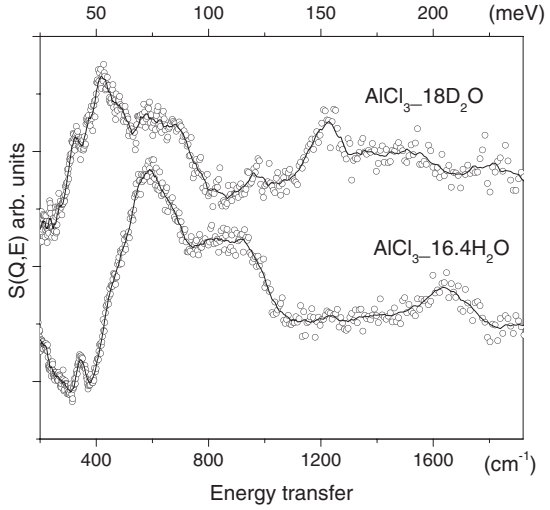

Figure 10. Inelastic neutron scattering spectra of concentrated aqueous solutions of aluminium chloride in ordinary pure water and in deuterium oxide ($18H_2O/Al^{3+}$) in the glassy state ($T < 25$ K). The solid curves represent the average of the data.

(2) If the ordinary water solvent is replaced by deuterium oxide, the following modifications are observed: a narrow, low intensity peak at 320–350 cm^{-1} (figures 10 and 11) is displaced about 25–35 cm^{-1} towards lower frequency. Secondly, in spectra of solutions in ordinary water, a wide, intense spectral band extending from about 350 cm^{-1} up to 1000 cm^{-1}, with a maximum at about 600 cm^{-1}, is also displaced to lower frequencies, but in this case the displacement is about 100–120 cm^{-1}. The peaks with the small isotopic shift (25–35 cm^{-1}) are attributed to predominantly translational vibrations of the water molecules belonging to the cation hydrates. The spectral bands with the larger isotopic shifts are assigned, obviously, to predominantly librational vibrations of the water molecules. These water molecules are water molecules belonging to the hydrate and *free* water molecules

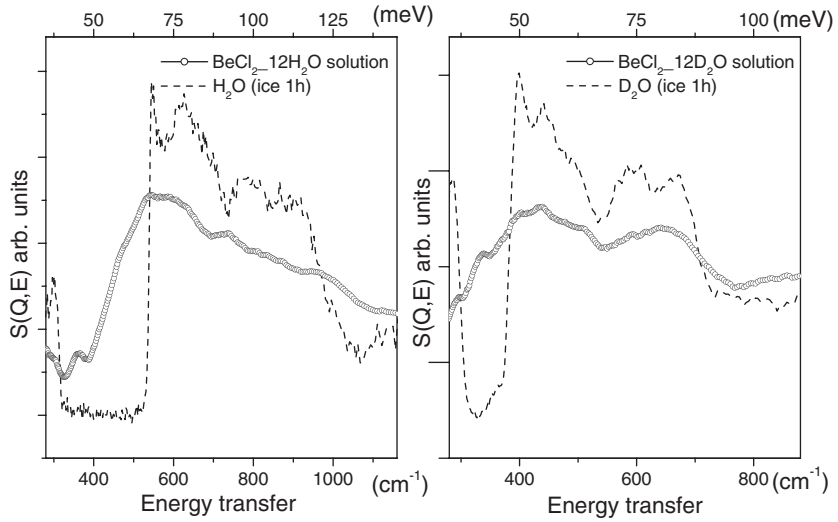

Figure 11. Inelastic neutron scattering spectra of concentrated aqueous solutions of beryllium chloride in ordinary pure water and in deuterium oxide ($12H_2O/D_2O$ per Be^{2+}) in the glassy state.

(we should emphasize that in very concentrated aqueous solutions the structure of these *free* water molecules should be different from the structure of pure water).

The isotopic shift observed for the 'librational' maxima of the inelastic neutron scattering spectra ($\sim$1.2) is smaller than that suggested from the ratio of the momentums of inertia of the water molecule about its centre of mass ($\sim$1.4). This may be due to the idea of possible coupling of translational and librational vibrations of *free* water molecule modes. The modification of the spectra in the region below $\sim$300 cm^{-1} is not analysed in this paper. A comparison of the spectra for aqueous solutions of aluminium chloride, bromide and beryllium chloride is given in figures 10 and 11 and their frequency values are presented in table 2.

(3) The effect of changing the concentration is shown in figure 12 for aluminium chloride and aluminium bromide and in figure 13 for beryllium chloride. The vertical lines in figure 12 indicate the frequency values at which the three Raman active bands assigned to the cation hydrate are observed. The relative intensity of the bands at $\sim$340 cm^{-1} decreased with increasing number of water molecules per cation, as expected from its assignment to one of the vibrational modes of the cation hydrate. In beryllium chloride solutions (figure 13) a slight increase of the frequency of the band ν_2 is observed, in agreement with the Raman spectral measurements. It is also supposed that librational vibrations of the coordinated water molecules occur in that spectral region.

An identification of individual vibrational modes in the inelastic neutron scattering spectra at frequencies greater than $\sim$400 cm^{-1} is not possible, due to the overlap of contributions from different vibrations associated with different water molecules and to the low statistical quality of the data. Despite this, the observation gives indications of the perturbations induced by the cation on the overall dynamics of the water molecules in solution. The librational vibrations that are assumed to couple with the totally symmetric contraction–dilation vibrations of the cation hydrates are included in the interval of intense inelastic neutron scattering of the aqueous solutions above $\sim$370 cm^{-1} shown in figures 10 and 11.

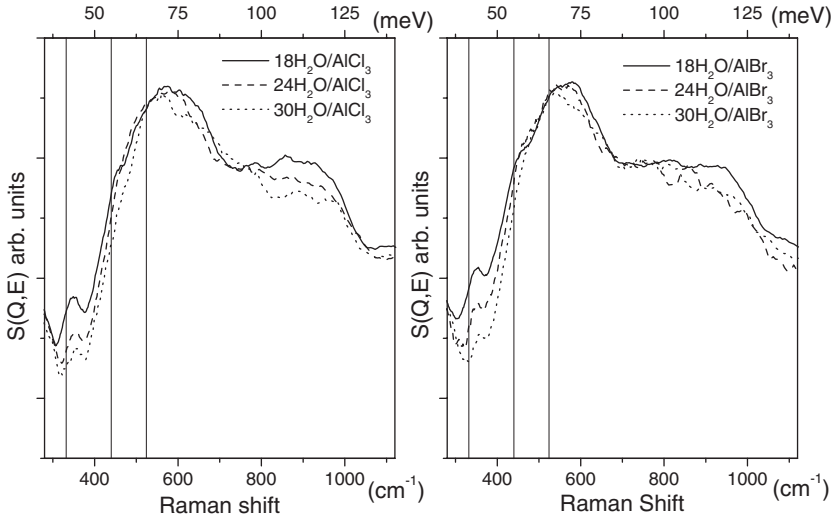

Figure 12. Inelastic neutron scattering spectra corresponding to different values of the concentrations of aqueous solutions of aluminium chloride and aluminium bromide in the glassy state ($T < 25$ K). See the caption of table 2.

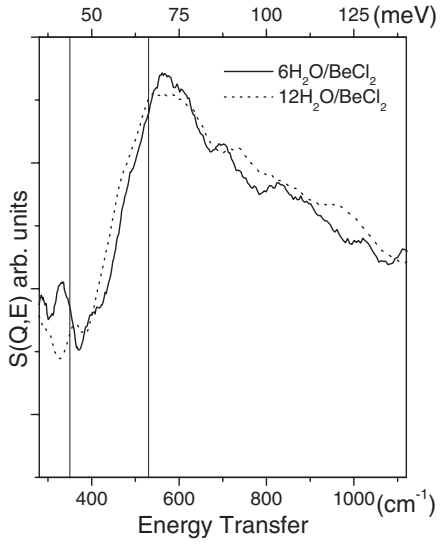

Figure 13. Inelastic neutron scattering spectra corresponding to different values of the concentration of beryllium chloride aqueous solutions ($6/12H_2O$ per Be^{2+}). The intensity of the band observed near 340 cm^{-1} diminishes when the value of the concentration lowers. A slight shift of the frequency towards the high value of the energy transfer is observed, too. See the caption of table 2.

3.3. X-ray diffraction investigations

The aim of these experiments is to obtain from the positional correlations of cation hydrates information about direct contact between them, which should support the idea of a possible coupling between the vibrational modes of these aggregates.

The possibility of existence of position correlations in aqueous solutions at distances that considerably exceed those corresponding to direct contact was first suggested by Prins [57] in 1935, to interpret a well defined intensity maximum at small diffraction angles ($Q \sim 1$ Å^{-1}), observed in the x-ray diffraction patterns of aqueous solutions of salts of heavy ions. This maximum, the *prepeak*, is not present in diffraction patterns of liquid water. With molten salts

and glasses the expression *first sharp diffraction peak* (FSDP) is used to refer to such maxima. The connection between the existence of a FSDP in the diffraction pattern of a non-crystalline material and the plausibility of an 'intermediate range order' has been discussed in a number of recent articles [58–66]. About thirty years after the article of Prins [57], correlations between heavy and light divalent cations in aqueous solutions of their chlorides were investigated by Skryshevski *et al* [67].

Two of the authors of this paper carried out x-ray diffraction experiments [5] on concentrated aqueous solutions of aluminium chloride, bromide etc, reported in 1974. From these preliminary experiments [5] it was concluded that:

(i) the water molecules in direct contact with the cation reinforce the intensity of the *prepeak*,
(ii) the value of Q corresponding to this *prepeak*, the maximum of intensity at $Q \sim 1$ Å^{-1}, diminishes when the concentration of the salt decreases (behaviour already observed by Prins) and
(iii) heavy anions, such as bromide ones, produce destructive interferences that in many cases prevent the observation of this *prepeak*.

The hypothesis of the existence of this *prepeak* for many other solutions has motivated us to continue a series of studies concerning a plausible interpretation of these interference maxima. A large number of aqueous solutions [5, 68–75] were investigated, and experiments on successive dilutions of the same solution (from almost saturated solutions down to $\sim$1 mol dm^{-3} concentrations) show the existence of positional correlations between cation hydrates in solutions of salts involving ions of different valences. For the solutions studied, each higher valence ion is surrounded, apparently, by a number of similar neighbours. These are at a large distance compared with the distance between the ions and the water molecules lying in direct contact [5]. Previous spectral observations have shown that the values of the frequency of the internal vibrations of the hydrate do not change with dilution. This experimental result as well as the hypothesis of the large value of the distance between the neighbour hydrates suggest that no coupling between the internal vibrations of neighbour hydrates is probable.

X-ray diffraction patterns of aqueous aluminium chloride and bromide solutions at the highest concentration studied in both liquid and glassy states are shown in figure 14, together with the corresponding pair correlation functions. Although the main maxima and minima appear sharper in the glassy state, the low temperature intensity profile is similar to that at room temperature. Similar results were obtained for more dilute solutions (table 1). The amplitude of the first maximum of the pair correlation functions obtained is in agreement with the presence of six water molecules in the hydration shell of the aluminium cation (figures 14(e), (f)). These results confirm the same hydration structures in the glassy and liquid aqueous solutions, as described above.

A *prepeak* is observed near 1 Å^{-1} in the diffraction patterns of aqueous aluminium chloride solutions, indicating positional correlations at distances greater than those for direct contact. The evolution of this maximum with concentration is given in figure 15. The values of Q corresponding to the maxima indicated seem to be proportional to the one-third power of the molar concentration (see the inset). From the slope of the straight line, these observations are consistent with the existence of a *liquid-type quasi-close packing* (LTQCP) of cation hydrates in aqueous aluminium halide solutions. In the same figure, the straight line corresponding to the existence of a simple cubic distribution of cations is also shown. Similar structural order has already been suggested to interpret the x-ray diffraction patterns of concentrated aqueous solutions of other salts [68–75]. In the majority of the cases, face-centred cubic (fcc) packing is considered only for the first-neighbour distances. Here, hydrated cations are positioned with respect to each other at the maximal distance allowed by the volume available

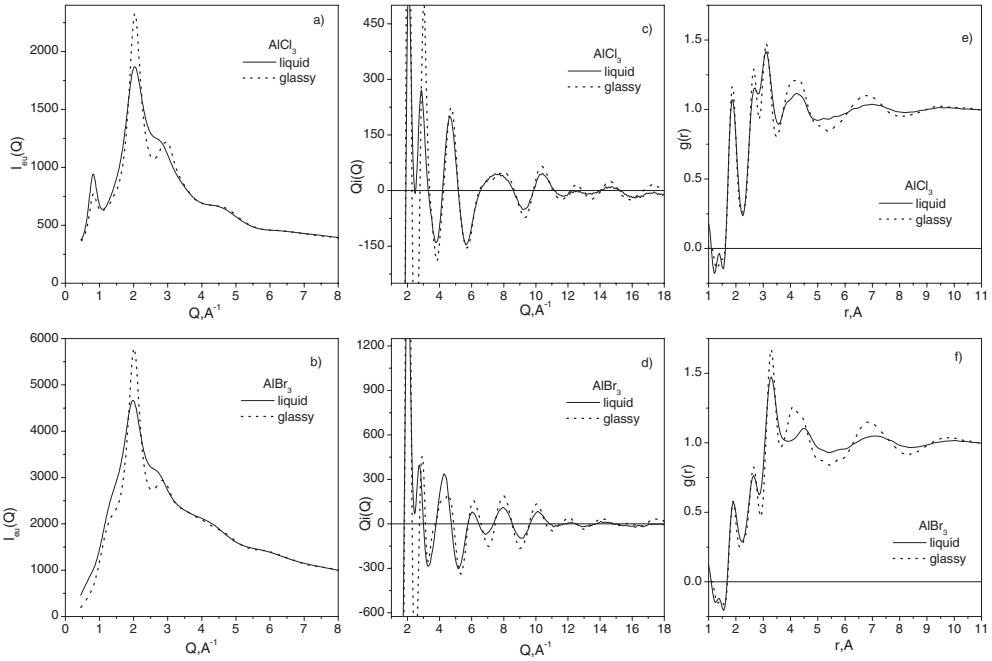

Figure 14. X-ray experimental data of concentrated aluminium chloride and aluminium bromide aqueous solutions ($18H_2O/Al^{3+}$) in liquid ($T = 295$ K) and glassy ($T = 25$ K) states. ((a), (b)) $I_{eu}(Q)$; ((c), (d)) $Qi(Q)$; ((e), (f)) pair correlation functions $g(r)$.

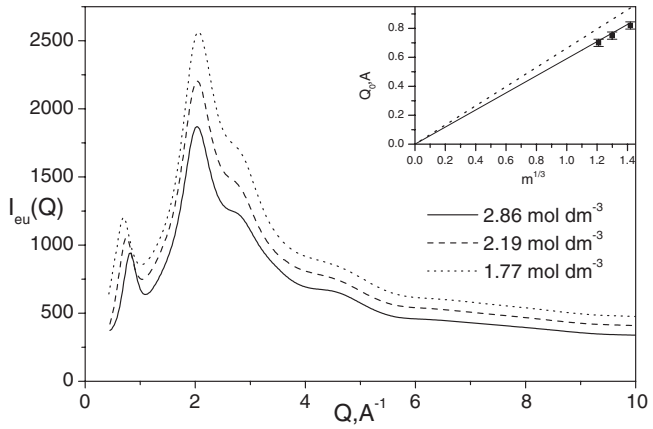

Figure 15. X-ray diffraction patterns of aluminium chloride aqueous solutions in different concentrations. The value of Q_0 (the abscissa of the *prepeak*) would be proportional, in ideal conditions, to the power 1/3 of the value of the molar concentration, if the hydrated cations are assumed as ordered in a face-centred cubic (solid line) or in a simple cubic (dotted line) lattice, both represented in the inset. The experimental points corresponding to the three solutions investigated coincide approximately with the solid line (face-centred cubic lattice).

in a hypothetical cubic arrangement. This leads to a maximum number of water molecules coordinated by the cation (the ion of highest electric charge). This seems to be a consequence of the large electric charge of the cation compared with that of the anion, resulting in intense

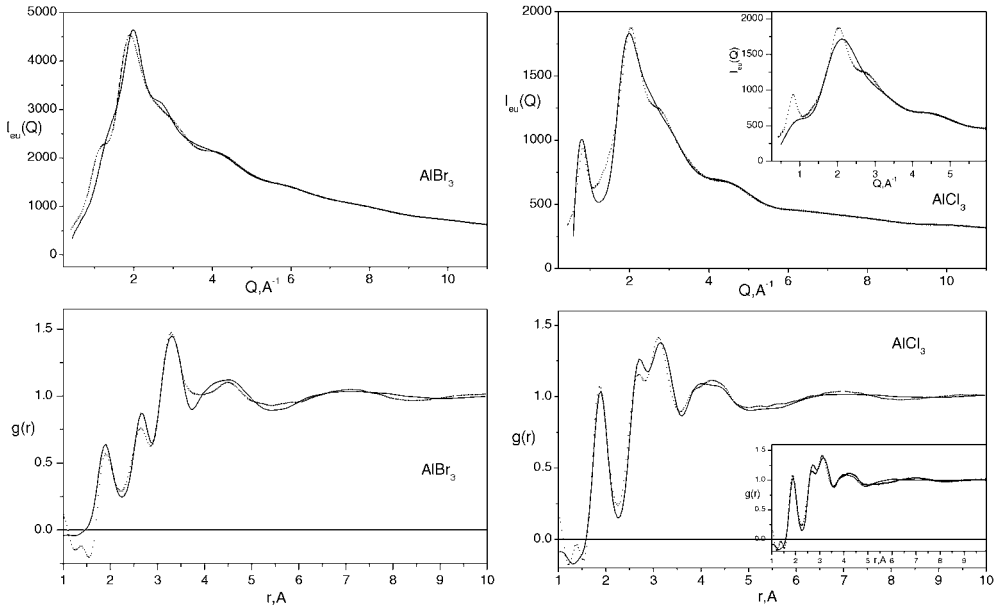

Figure 16. Molecular models of the 2.86 mol dm^{-3} aluminium chloride and the 2.67 mol dm^{-3} aqueous solutions. Intensities $I_{\mathrm{eu}}(Q)$ and the pair correlation function are displayed: calculated from the model (——) and experimental (+ + ++). The insets show the curves calculated from a model without LTQCP (see the text and table 3).

cation–cation electrostatic repulsion. The intensity maximum at $Q \sim 1$ Å^{-1} depends on the contrast between the density of the scattering power of the molecular *cloud* centred in the high valence ion and the mean value corresponding to the solution. The fitting of the scattering power to reproduce reasonably well the real value requires that the number of first-neighbour cations (here the ions of larger valence), contributing to the quasi-close packing, be adjusted. This number has been, as a rule, smaller than twelve, because the diffusive motion of the water molecules surrounding the ions of larger valence disturbed a hypothetical *strict* local order in the ionic solutions investigated. The use of the expression *liquid-type quasi-close packing* indicates, finally, that a true close packing order cannot be considered beyond the first shell because (1) the values of the fluctuations of the distances between the centres of the *marshalled clouds* increase quickly and (2) the lifetimes of these *clouds* are very short. But we must emphasize that the distances between first neighbours are calculated from an isotropic close packing (fcc) having the same number density as that of the solution.

The position of the anions is relevant to the diffraction pattern, in the low Q region (<2 Å^{-1}) (figures 14(a), (b)). In particular, at $Q \sim 1$ Å^{-1}, a *prepeak* is not observed in the diffraction pattern of aqueous aluminium bromide solution (figures 14(b) and 16). This is not in disagreement with the existence of a *liquid-type quasi-close packing*, LTQCP. Electrostatics suggests that in these concentrated aqueous solutions the anions are located roughly at the mid-points of the cation–cation distance and hence contribute destructively to the intensity of the *prepeak*. Because of the increase in the anion scattering power, a large reduction or even disappearance of this *prepeak* would then be expected when replacing the chloride anion by the bromide anion in aqueous solution.

So the structure of aqueous aluminium chloride and bromide at the highest concentration was simulated assuming the hypothesis of a LTQCP structure for calculating the x-ray

diffraction patterns and the pair correlation functions. The method of calculation has previously been described in detail [5, 68, 69], and only the main guidelines will be presented in appendix B.

The calculated intensities $I_{eu}(Q)$ and pair correlation functions $g(r)$ are shown in figure 16 for aqueous aluminium chloride and bromide solutions at the highest concentration at room temperature. The positional correlations used in these calculations are given in table 3. As discussed above, a LTQCP of cation hydrates, each constituted by six water molecules in an octahedral arrangement around the cation, was assumed. On average, anions were surrounded by six water molecules, some belonging to the hydration shells of the neighbouring cations (table 3: *water(h)–anion* and *anion–water(f)*). The other water molecules were distributed in the available free space, in the holes of the local close packing.

The similarity of the structural arrangement, that were found to agree reasonably well with the experimental intensities of the aqueous aluminium chloride and bromide solutions, demonstrates the role of the scattering power of the anions, through the observed differences between the diffraction patterns of the two aqueous halide solutions.

It should be noted that a good simulation of the diffraction patterns in the region of the *prepeak* could not be achieved if positional correlations beyond direct contact were not considered. For example, the profile obtained for aqueous aluminium chloride solution neglecting positional correlations between cation hydrates, and restricting the discrete part of the other correlations to the shortest distances, is shown in the inset of figure 16 (see also table 3).

4. Conclusion

The similar results obtained for the liquid and the glassy states by Raman, x-ray diffraction and inelastic neutron scattering investigation of the concentrated aqueous solutions studied supports the existence of similar hydration structures in both states.

Raman experiments on concentrated aqueous solutions of aluminium and beryllium halides in liquid and glassy states confirm previous results obtained at room temperature on aqueous solutions of the same salts. The isotope shifts observed in the neutron and Raman spectra of light and heavy water solutions can be explained by assuming a coupling between the translational and librational motions of the water molecules belonging to the cation hydrates. Inelastic neutron scattering experiments seem to confirm Raman results, such as the existence of similar vibrational spectra of the different halides of the same cation (a minor role is played by anions in the vibrational structure of the cation hydrates).

X-ray diffraction experiments with solutions of different concentrations of the same salt provided information on positional correlations between the cation hydrates. The molecular models developed are able to reproduce the main trends in the x-ray diffraction patterns of the concentrated aqueous solutions of aluminium chloride and bromide in Q-space and in r-space. The similarity of the positional correlations considered in the molecular models of the two halides in their aqueous solutions demonstrates the minor role played by the anion in the intermediate range order of these concentrated aqueous solutions. These models suggest the existence of a local arrangement of cation hydrates in a *liquid-type quasi-close packing*.

Acknowledgments

The authors would like to thank Maria Clara Carreiro da Costa, who prepared and analysed the solutions. Professor A M Amorim da Costa and Dr M Paula Marques were available

Table 3. More relevant positional correlations considered in the molecular models of the aqueous solutions of $AlCl_3$ and $AlBr_3$ (whose calculated curves are represented in figure 16). Distances are in Å. r, mutual distances; Δr, rms; w, weight; r_{th}, threshold distance. The values underlined correspond to the internal positional correlations of the cation hydrates.

	$AlBr_3$				$AlCl_3$							
	LTQCP				LTQCP				No long range			
Correlations	r	Δr	w	r_{th}	r	Δr	w	r_{th}	r	Δr	w	r_{th}
Cation–cation	9.6	1.0	6	10.2	9.3	1.0	6	9.9				5.2
Cation–water(h)	1.90	0.08	12		1.90	0.08	12		1.90	0.08	12	
	7.7	0.8	12		7.4	0.8	12					
	8.4	0.9	12		8.1	0.9	12					
	9.8	1.0	48	10.2	9.5	1.0	48	9.9				5.2
Water(h)–water(h)	2.66	0.08	24		2.66	0.08	12		2.66	0.08	6	
	3.76	0.11	6		3.76	0.11	6		3.76	0.11	6	
	5.8	0.6	3		5.7	0.6	3					
	6.5	0.7	12		6.3	0.7	12					
	...	...	...		...	...	...					
	7.9	0.8	36		7.7	0.8	36					
	...	...	...		...	...	...					
	9.6	1.0	24	8.9	9.3	1.0	24	8.7				5.2
Cation–anion	4.4	0.3	6		4.2	0.3	6		4.2	0.3	6	
	5.2	0.6	4.5	6.4	5.2	0.6	4.5	6.2				5.2
Water(h)–anion	3.3	0.2	12		3.2	0.2	12		3.2	0.2	12	
	4.1	0.3	9		4.0	0.3	9		4.0	0.3	9	
	4.7	0.4	12		4.6	0.4	12		4.6	0.4	12	
	5.7	0.6	21		5.6	0.6	21		5.4	0.6	9	
	6.7	0.6	9	6.4	6.6	0.6	9	6.2				5.2
Anion–anion	4.4	0.3	3		4.2	0.3	3		4.2	0.3	3	
	4.8	0.4	3		4.7	0.4	3		4.7	0.4	3	
	6.2	0.6	1.5		6.0	0.6	1.5					
	6.7	0.6	3	6.1	6.6	0.6	3	5.9				5.2
Cation–water(f)	3.8	0.2	6		3.8	0.2	6		3.8	0.2	6	
	5.3	0.6	22		5.1	0.6	22		5.1	0.6	18	
	5.9	0.6	20		5.7	0.6	20		5.7	0.6	4	
	6.2	0.6	12		6.0	0.6	12					
	7.0	0.6	16	7.6	6.8	0.6	16	7.4				5.2
Water(h)–water(f)	2.7	0.1	12		2.7	0.1	12		2.7	0.1	12	
	...	...	...		...	...	...		...	...	...	
	5.1	0.6	64		4.9	0.6	64		4.9	0.6	64	
	...	...	...		...	...	...					
	6.1	0.6	60	6.6	5.9	0.6	60	6.4				5.2
Anion–water(f)	3.3	0.2	18		3.2	0.2	18		3.2	0.2	18	
	3.5	0.2	6		3.4	0.2	6		3.4	0.2	6	
	...	...	...		...	...	...		...	...	...	
	5.0	0.6	12		5.0	0.6	12		5.0	0.6	12	
	...	...	...		...	...	...					
	6.1	0.6	24		6.0	0.6	24					
	7.3	0.8	60	7.0	7.1	0.8	60	6.8				5.2
Water(f)–water(f)	2.8	0.1	32		2.8	0.1	32		2.8	0.1	32	
	3.6	0.2	24		3.5	0.2	24		3.5	0.2	24	
	...	...	...		...	...	...		...	...	...	
	5.8	0.6	24		5.8	0.6	24		5.8	0.6	4	
	...	...	...		...	...	...					
	6.8	0.7	12	6.2	6.6	0.7	12	6.0				5.2

Table 4. Calculated values of the frequency of the internal oscillational modes of the cation hydrate; Raman active, approximately simulated by a coupling between an internal purely translational mode of the hydrate and a pure librational motion of the coordinated water molecule. Numerical values of the frequency are in cm^{-1}. $\left(\text{Note: } \xi'^2_{t,l} = \frac{\xi_t^2+\xi_l^2}{2} \pm \sqrt{\frac{(\xi_t^2-\xi_l^2)^2}{4} + \chi\xi_t^2\xi_l^2}.\right)$

χ	$\xi_t^{H_2O}$	$\xi_l^{H_2O}$	$\xi_t^{D_2O}$	$\xi_l^{D_2O}$	$\xi_t'^{H_2O}$	$\xi_l'^{H_2O}$	$\xi_t'^{D_2O}$	$\xi_l'^{D_2O}$	$\xi_t^{H_2O}/\xi_t^{D_2O}$
Totally symmetric vibrations									
0.003	530	570	503	425.4	524.8	574.8	504.8	423.2	1.040
0.010	530	570	503	425.4	515.0	583.3	508.8	418.4	1.012
0.003	530	630	503	470.1	527.3	632.2	507.5	465.2	1.039
0.010	530	630	503	470.1	521.5	637.0	515.3	456.6	1.012
0.003	530	710	503	507.1	528.2	711.3	490.9	518.8	1.076
0.003	530	960	503	685.7	528.9	960.6	501.4	686.9	1.055
Degenerate vibrations									
0.02	350	570	332	425.4	344.4	573.4	431.5	324.0	1.063
0.02	350	630	332	470.1	345.0	632.8	474.5	325.6	1.060

for assistance in preliminary Raman experiments in the Laboratório de Espectroscopia de Raman do Departamento de Química da Universidade de Coimbra. Dr Matthew Hallshall is acknowledged for providing the Raman facilities. Dr John Finney created the conditions for the authors' access to ISIS (RAL), which were supported by a grant under the European Union (Improvement of Human Potential) programme. Dr Stewart Parker and Dr Daniele Colognesi are thanked for their assistance with the inelastic neutron scattering experiments and Dr F Margaa's participation in preliminary inelastic neutron scattering experiments is acknowledged. Dr Thomas Buslaps and Dr Veijo Honkimaki are acknowledged for their assistance before and during the x-ray diffraction experiments at ESRF. Professor H D Burrows of Universidade de Coimbra is thanked for reading the manuscript. Ana Gaspar acknowledges the financial support given by 'Fundao para a Cincia e Tecnologia' in the form of a PhD grant (BD/21411/99). 'Fundaçao Luso-Americana' is also thanked for funding the participation of the first two authors in international conferences held in the United States.

Appendix A

The knowledge of the structure of the water molecule does not allow accurate estimation of the value either of the frequency of the librational modes or of the coupling parameters with the translational modes (with frequency values close to the corresponding polarized Raman bands u1 of the cation hydrates). A range of numerical values for the quantities referred to are suggested as paradigmatic examples, which allow calculation of values of the isotopic shifts in agreement with experiment. So couplings at each step of only two (vibrational) modes, one being purely translational and another one librational, were successively considered to calculate the values of the isotopic shifts. The global result is obtained by the cooperation of the effects of each step. As the values of the coupling parameters are small the different effects may be, approximately, considered as additive.

ξ_l is the frequency value of a purely librational mode,

ξ_t is the frequency value of a purely translational mode,

ξ_l' is the frequency value of the predominantly librational mode obtained by the coupling of the vibrational mode corresponding to $\xi_l^{H_2O}$ with the mode corresponding to $\xi_t^{H_2O}$,

ξ_t' is the frequency value of the predominantly translational mode obtained by the coupling described,

χ is the value of the coupling parameter.

The values of $\xi_l^{H_2O}$ in the first four rows of table 4 are in the interval (550–650 cm^{-1}). These data allow determination of the vibrational frequencies resulting from the coupling with the purely translational mode ξ_t, values ξ_t' that lead to isotopic shifts ratios smaller than 1.054, in agreement with the Raman experiments.

The values of $\xi_l^{H_2O}$ in the following two rows are outside of this interval. They are suggested to be representative of other librations, such as rocking and twisting vibrations that differ from the wagging vibrations. They may eventually couple with the purely translational contraction–dilation ξ_t of the hydrates but, according to our hypothesis of a preferential coupling with wagging vibrations, only to a small extent.

The values $\xi_l^{D_2O}$ in the first four rows were fixed in agreement with the ratio $\xi_l^{H_2O}/\xi_l^{D_2O} = 1.34$. This is the ratio of the moments of inertia I^{D_2O} and I^{H_2O} of the molecules D_2O and H_2O (about the centre of mass) in the wagging motion. $\xi_l^{D_2O}$ in the following two rows were fixed as $I^{D_2O}/I^{H_2O} = 1.40$ (the ratio of the moments of inertia of the molecules D_2O and H_2O is, for the rocking and twisting librations, respectively 1.39 and 1.41).

The values $\xi_t^{H_2O}$ and $\xi_t^{D_2O}$ are considered as representative of the purely translational motions that are assumed as coupled with purely librational motions ξ_l. The ratio $\xi_t^{H_2O}/\xi_t^{D_2O}$ is in agreement with the values of the molecular masses of D_2O and H_2O and has, obviously, the value 1.054.

The suggestion of the coupling with librational oscillations of the purely translational motions ω_2 and ω_3 of the water molecules of the cation hydrates is checked by using the value 350 cm^{-1} for $\xi_t^{H_2O}$ in the last two rows of table 4.

The cooperation of the three modifications produced in the values of $\xi_t^{H_2O}$ and $\xi_t^{D_2O}$ by the three couplings with the three librational modes (using appropriate parameters) must be used for the comparison with the results of the Raman experiments, as was indicated above.

Values of the coupling parameter, χ, larger than those that are indicated for the totally symmetric vibrational modes are suggested for the degenerate modes ω_2 and ω_3 because in these vibrations a more intense coupling with different librational modes seems acceptable.

Appendix B

The dependent intensity corresponding to the molecular model is calculated using the Debye formula:

$$i(Q) = \sum_{j \neq k} f_j f_k \frac{\sin(Q r_{jk})}{Q r_{jk}} \tag{4}$$

where f_j are the ionic or molecular scattering factors and r_{jk} the distances between the ions or molecules j and k. The validity of this approximation is based on the spherical symmetry around each atom or molecule, approximately fulfilled on average within the volume of coherence of the Rayleigh scattering.

In the sum, the discrete region is intended to simulate the local order around each particle j for which the local density is different from the bulk density. These differences attenuate for increasing values of distances r. For distances above a given threshold r_{jl}^{th} the discrete distribution of distances is replaced by a continuous uniform distribution. This approximation, certainly inappropriate, leads to some uncertainty in the value of the calculated intensity when the term corresponding to the continuous is of the order of the term that comes from the discrete distribution. For that reason, the calculated curves presented in each figure from 0.5 $Å^{-1}$ are

only reliable above 0.7 $Å^{-1}$. Fluctuations of the distances between ions and molecules within the discrete region as well as of the continuum thresholds are assumed (arbitrarily) to be Gaussian, and are appropriately adjusted for each aqueous solution.

References

[1] da Silveira A 1932 *C. R. Acad. Sci.* **194** 1336 and references therein
[2] da Silveira A, Alves Marques M and Macias Marques N 1961 *C. R. Acad. Sci.* **252** 3983
da Silveira A, Alves Marques M and Macias Marques N 1965 *Mol. Phys.* **9** 271
[3] Alves Marques M 1960 *Thesis* Universidade Te'cnica de Lisboa
[4] Irish D E 1971 *Ionic Interactions* ed S Petrucci (New York: Academic) p 220
[5] Alves Marques M and de Barros Marques M I 1974 *Proc. K. Ned. Akad. Wet.* B **77** 286
[6] Colognesi D, Celli M, Newport R J, Parker S F, Rossi-Albertini V, Sacchetti F, Tomkinson J and Zoppi M 2002 *Appl. Phys.* **74** 564
[7] Maslen E N, Fox A G and O'Keefe M A 1992 *International Tables of Crystallography* vol C, ed A J C Wilson (London: Kluwer–Academic) chapter 6
[8] Cromer D T and Liberman R 1970 *J. Phys. Chem.* **53** 1891
Kissel L, Zhou B, Roy S C, Gupta S K and Pratt R H 1995 *Acta Crystallogr.* A **51** 271
[9] Palinkas G and Radnai T 1976 *Acta Crystallogr.* A **32** 666
[10] Cromer D T and Mann J B 1968 *Acta Crystallogr.* A **24** 321
[11] Hajdu F 1972 *Acta Crystallogr.* A **28** 250
[12] Krogh-Moe J 1956 *Acta Crystallogr.* A **9** 951
Norman N 1957 *Acta Crystallogr.* A **10** 370
[13] Warren B E 1968 *X-ray Diffraction* (Reading, MA: Addison-Wesley) p 116
[14] Connick R E and Fiat D N 1963 *J. Chem. Phys.* **39** 1349
[15] Swift T J and Sayre W G 1966 *J. Chem. Phys.* **44** 3567
[16] Fratiello A, Lee R E, Nishida V M and Schuster R E 1968 *J. Chem. Phys.* **48** 3705
[17] Yamaguchi T, Ohtaki H, Spohr E, Palinkas G and Heinzinger K 1986 *Z. Naturf.* a **46** 1986
[18] Jackson J A, Lemons J F and Taube H 1960 *J. Chem. Phys.* **32** 553
[19] Matwiyoff N A, Darley P E and Movious M G 1968 *Inorg. Chem.* **7** 2173
[20] Schuster R E and Fratiello A 1967 *J. Chem. Phys.* **47** 1554
[21] Bol W and Welzen T 1977 *Chem. Phys. Lett.* **49** 189
[22] Caminiti R, Licheri G, Piccaluga G, Pinna G and Radnai T 1979 *J. Chem. Phys.* **71** 2473
Caminiti R and Radnai T 1980 *Z. Naturf.* a **35** 1368
[23] Takahashi A 1968 *J. Phys. Soc. Japan* **24** 657
Takahashi A 1970 *J. Phys. Soc. Japan* **28** 207
[24] Hugi-Cleary D, Helm L and Merbach A E 1985 *Helv. Chim. Acta* **68** 545
[25] Van der Maarel J R C and Bleijser J 1987 *Chem. Phys. Lett.* **141** 251
[26] Herdman G J and Neilson G W 1990 *J. Mol. Liq.* **46** 165
[27] Kanno H 1988 *J. Phys. Chem.* **92** 4232
[28] Alves Marques M, Sousa Oliveira M A and Resina Rodrigues J 1990 *J. Chem. Soc. Faraday Trans.* **86** 471
[29] Rudolph W W, Mason R and Pye C C 2000 *Phys. Chem. Chem. Phys.* **2** 5030
Rudolph W W and Schonherr S 1991 *Z. Phys. Chem.* **173** 167
Rudolph W W and Schonherr S 1989 *Z. Phys. Chem. Lpz.* **270** 1121
[30] Bergstrom P, Lingren J, Read M and Sandstrom M 1995 *J. Phys. Chem.* **91** 7650
[31] Hermansson K H and Olovsson I 1984 *Theor. Chim. Acta* **64** 265
[32] Marcos E S, Papallardo R R and Rinaldi D 1991 *J. Phys. Chem.* **95** 8928
[33] Floris F, Persico M, Tani A and Tomasi J 1995 *Chem. Phys.* **195** 207
[34] Wassernan E, Rustad J R and Xantheas S 1997 *J. Chem. Phys.* **106** 9769
[35] Kubiki J D, Sykes D and Apitz S E 1999 *J. Phys. Chem.* A **103** 903
[36] Martinez J M, Pappalardo R R and Sanchez Marcos E 1999 *J. Am. Chem. Soc.* **121** 3175
[37] Bakker A, Hermansson K, Lindgren J, Probst M M and Bopp P A 1999 *Int. J. Quantum Chem.* **75** 660
[38] Lubin M I, Bylaska E J and Weare J H 2000 *Chem. Phys. Lett.* **322** 447
[39] Ikeda T, Hirate M and Kimura T 2003 *J. Chem. Phys.* **119** 12386
[40] Spangberg D and Hermansson K 2004 *J. Chem. Phys.* **120** 4829
[41] Corongiu C and Clementi E 1978 *J. Chem. Phys.* **69** 4885
[42] Markham G D, Glusker J P, Block C L, Tachtman M and Bock C W 1996 *J. Phys. Chem.* **100** 3488

[43] Katz A K, Glusker J P, Beebe S A and Bock C W 1996 *J. Am. Chem. Soc.* **118** 5752
[44] Marx D, Sprik M and Parinello M 1997 *Chem. Phys. Lett.* **273** 360
[45] Pavlov M, Sieghbahn P E M and Sandstrom M 1998 *Phys. Chem.* A **102** 219
[46] Magat M 1936 *Ann. Phys. Fr.* **6** 108
[47] Walfaren G E 1972 *Water: A Comprehensive Treatise* vol I, ed F Franks (New York: Plenum) p 151
[48] Neilson G W and Enderby J E 1978 *J. Phys. C: Solid State Phys.* **11** L625
Newsome J R, Neilson G W, Enderby J E and Sandström M 1981 *Chem. Phys. Lett.* **82** 399
Powell D H and Neilson G W 1990 *J. Phys.: Condens. Matter* **2** 3871
[49] Neilson G W and Newsome J R 1981 *J. Chem. Soc. Faraday Trans.* **77** 1245
Salmon P S, Neilson G W and Enderby J E 1988 *J. Phys. C: Solid State Phys.* **21** 1335
[50] Newsome J R, Neilson G W and Enderby J E 1980 *J. Phys. C: Solid State Phys.* **13** L923
Sandstrom M, Neilson G W, Johansson G and Yamaguchi T 1985 *J. Phys. C: Solid State Phys.* **18** L1115
[51] Cummings S, Enderby J E and Howe R A 1980 *J. Phys. C: Solid State Phys.* **13** 1
Hewish N A, Neilson G W and Enderby J E 1982 *Nature* **297** 138
[52] Narten A H and Hahn R L 1983 *J. Phys. Chem.* **87** 3193
Biggin S, Enderby J E, Hahn R L and Narten A H 1984 *J. Phys. Chem.* **88** 3634
Annis B K, Hahn R L and Narten A H 1985 *J. Chem. Phys.* **82** 2086
Cossy C, Barnes A and Enderby J R 1989 *J. Chem. Phys.* **90** 3254
Yamaguchi T, Tanada S, Wakita H, Misawa H, Okada I, Soper A K and Howells W S 1990 *Z. Naturf.* a **46** 84
[53] Herdman G J and Neilson G W 1992 *J. Phys.: Condens. Matter* **2** 627
Herdman G J and Neilson G W 1992 *J. Phys.: Condens. Matter* **2** 649
[54] Broadbent R D, Neilson G W and Sandstrom M 1992 *J. Phys.: Condens. Matter* **4** 639
[55] Teixeira J, Bellissent-Funel M C, Chen S H and Dianoux A J 1985 *Phys. Rev.* A **31** 1913
Ullo J J 1987 *Phys. Rev.* A **36** 816
[56] Li J-C and Kolesnikov A I 2002 *J. Mol. Liq.* **100/101** 1
[57] Prins J A and Fonteyne R 1935 *Physica* **2** 1016
Prins J A and Fonteyne R 1935 *J. Chem. Phys.* **3** 72 and references therein
[58] Iijima T and Nishikawa K 1985 *Chem. Phys. Lett.* **115** 522
[59] Moss S C and Price D L 1985 *Physics of Disordered Materials* ed H D Adler, H Fritzsche and S R Ovshinsky (New York: Plenum) p 77
[60] Price D L, Moss S C, Reijers R, Saboungi M L and Susman S 1989 *J. Phys.: Condens. Matter* **1** 1005
[61] Penfold I T and Salmon P S 1991 *Phys. Rev. Lett.* **67** 97
[62] Salmon P S 1992 *Proc. R. Soc.* A **437** 591
[63] Elliot S R 1992 *J. Phys.: Condens. Matter* **4** 7661 and references therein
[64] Tosi M P, Price D L and Saboungi M L 1993 *Annu. Rev. Phys. Chem.* **44** 173
[65] Salmon P S 1994 *Proc. R. Soc.* A **445** 351
[66] Tosi M P 1999 *J. Mol. Liq.* **83** 23 and references therein
[67] Dorosch A K and Skryshevskii A F 1967 *Zh. Strukt. Khim.* **7** 348
[68] de Barros Marques M I, Cabaço M I, de Sousa Oliveira M A and Alves Marques M 1982 *Chem. Phys. Lett.* **91** 222
de Barros Marques M I 1983 *Thesis* Universidade de Lisboa
[69] Alves Marques M and Cabaço M I 1986 *Chem. Phys. Lett.* **123** 73
Alves Marques M, Cabaço M I and Sousa Oliveira M A 1986 *Chem. Phys. Lett.* **126** 551
Cabaço M I 1988 *Thesis* Universidade Te'cnica de Lisboa
[70] Cabaço M I, Alves Marques M, de Barros Marques M I, Bushnell-wye G, Costa M M R, de Almeida M J and Andrade L C 1995 *J. Phys.: Condens. Matter* **7** 7409
[71] Cabaço M I, Gaspar A M, de Morais C M and Alves Marques M 2000 *J. Phys.: Condens. Matter* **12** 2623
[72] Alves Marques M, Cabaço M I, de Barros Marques M I, Gaspar A M and de Morais C M 2001 *J. Phys.: Condens. Matter* **13** 4367
[73] Alves Marques M, Cabaço M I, de Barros Marques M I and Gaspar A M 2002 *J. Phys.: Condens. Matter* **14** 7427
[74] Alves Marques M, de Barros Marques M I, Cabaço M I, Gaspar A M and Almeida M L 2004 *J. Mol. Liq.* **110** 23
[75] Gaspar A M, Alves Marques M, Cabaço M I, de Barros Marques M I, Buslaps I and Honkimaki V 2004 *J. Mol. Liq.* **110** 15